Impedimetry and microscopy of electrosynthetic poly(propylene thiophenoimine)-co-poly(3,4 ethylene dioxythiophene) dendritic star copolymer

Rasaq A Olowu, Avril Williams, Peter M. Ndangili, Rachel F Ngece, Stephen N Mailu, Priscilla Baker, Emmanuel Iwuoha∗

SensorLab, Department of Chemistry, University of the Western Cape, Bellville, 7535, South Africa

∗E-mail: eiwuoha@uwc.ac.za

The electrochemical impedance spectroscopy of generation 2 poly(propylene thiophenoimine)-co-poly(3,4 ethylene dioxythiophene) dendritic star copolymer (G2PPT-co-PEDOT) film was studied in $LiClO_4$ solution. The results show that the electrochemical deposition of G2PPT-co-PEDOT on gold electrode decreased the electrochemical charge transfer resistance when compared to Au|PEDOT|$LiClO_4$ and Au|$LiClO_4$ interfaces. This is attributed to an increase in the conjugation length of the polymer as result of the linking of the highly conjugated PEDOT to the dendrimer. Bode impedimetric analysis indicates that G2PPT-co-PEDOT is a semiconductor with a maximum phase angle shift of $67.5°$ at 100 mHz. The star copolymer exhibited a 2-electron electrochemistry and a surface coverage of 97.3%. The morphology of the dendritic star copolymer was investigated by scanning electron microscopy and atomic force microscopy.

Keywords: Electrochemical impedance spectroscopy, conducting polymer, atomic force microscopy, scanning electron microscopy, dendritic star copolymer, nanomaterials, PEDOT.

1. INTRODUCTION

Over the past twenty years the field of π-conjugated polymers has attracted the attention of many scientists due to the interesting electrical and optical properties of these compounds [1]. In the class of intrinsically and electrically conducting polymers, poly(3,4 ethylene dioxythiophene), PEDOT, has been of interest in numerous studies due to its high conductivity, low oxidation state, excellent environmental stability and relatively low band gap [2]. These properties make it suitable for various applications such as electrochromic, light emitting diodes, capacitors [3] and sensors [4-5]. Conductive polymers may be employed in their unmodified state or they may be doped to enhance

1856

their electrical capability. PEDOT is one of the few examples of the conjugated polymer family that are both p-and n-dopable [6]. It is acknowledged that upon electrochemical p-doping (n-doping) conducting polymers undergo redox processes involving ion transport into and out of the polymer matrix to balance the electronic charge. This results not only in an increase in electronic conductivity, but also structural transition which gives rise to spectral changes [7-9]. The color exhibited by the polymer is determined by the band gap energy, defined as the onset of the $\pi-\pi*$ transition [10]. In order to diversify the properties and expand the function of classical $\pi-$conjugated polymer, copolymerization of the conducting polymer leading to a new material with modulated properties can be employed [11-12]. Synthesis of conducting polymer composites, graft and block copolymers have been established to be useful in compensating for some deficiencies of conducting polymers, such as poor mechanical and physical properties [12-13]. Electrochemical copolymerization can produce a variety of conducting materials with different optical, electrical and morphological properties as well as control electrochromic properties [12-14].

Dendritic polymers belong to a new class of synthetic macromolecules possessing a regular branched tree-like structure whose conduction path is along the π-stack [15-18]. The π-stack are formed in contrast to the traditional conducting polymer where the conducting path is based on alternating the single and double bond p-conjugated organic system [15]. Dendritic polymer conductivity is isotropic rather than anisotropic as usually observed in other conductive layered systems because the dendritic structure can form the p-stack in three dimensions. The field of dendrimer has been expanded greatly in recent years due to their justifiable assurance of being used in variety of applications. One of the progress in dendrimer based sensor system is the use of hybrid dendrimer containing encapsulated metal or the preparation of dendritic star copolymer which makes them useful for application in catalysis and electrocatalysis [19-20]. The formation of dendritic star copolymer with conducting polymers such as polyaniline, polythiophene and polypyrrole result in lead to the nanostructurization of the product due to elongation of the conjugation chain and unhindered π stacking of the polymer molecule by the dendrimer [20-21]. It also leads to improved processibility and electrical conductivity of the product [22-23]. When compared to linear chain polymer, spherical polymers can provide a material with reduced viscosity and melting point, higher solubility and enhanced substrate penetration as coating. Dendrimeric star copolymers are novel type of molecular architectures in which many linear homo or block copolymer chains are attached to a dendrimer core [22, 24]. The preparation of dendrimer-star

copolymer involves 2 general processes. The first process involves linking a monofunctional linear polymer onto the dendrimer surface [23], while the other process involves the growth of arm polymer chain from the surface of dendrimer by 'controlled/living' polymerizations such as anionic polymerization [24], ring-opening polymerization (ROP) [25], and atom transfer radical polymerization (ATRP) [26]. Synthesis of hybrid dendrimer-star copolymer through the reversible addition-fragmentation transfer (RAFT) polymerization process has been reported by Zheng and his coworker [27-28]. Wang and his coworkers reported a conducting star- shaped copolymer consisting of a regioregular poly(3-hexylthiopene) arm attached to a polyphenylene dendrimer core [29]. Miller and Tomalia [15] reported the conductivity of polyamidoamine (PAMAM) dendrimers modified with cationically substituted naphthalene diimides. This work for the first time (to the best of our knowledge) reports the synthesis, impedimetry and morphological characterization

Int. J. Electrochem. Sci., Vol. 6, 2011

1857

of novel conducting star copolymer composed of G2PPT dendrimer core and PEDOT arms grown at the α-positions of the dendrimer's thiophenoimine end groups.

2. EXPERIMENTAL SECTION

2.1. Materials and methods

A three electrodes cell with gold, platinum and Ag/AgCl (3 M NaCl type) as working, auxiliary and reference electrodes respectively was used. All voltammetric experiments were performed with Zahner IM6ex Germany. Electrochemical impedance spectroscopy (EIS) measurements were also recorded with Zahner IM6ex Germany, at perturbation amplitude of 10 mV within the frequency range of 100 kHz - 100 mHz.

The morphology of the samples was studied by scanning electron microscopy (SEM). SEM images were captured using a scanning electron microscope fitted with energy-dispersive X-ray spectroscopy accessory (Gemini LEO 1525 model microscope). SEM was carried out using screen printed carbon electrode (SPCE) as the substrate instead of gold electrode. $_1$H NMR (200 MHz) (Varian GerminiXR200 spectrometer), was carried out using deuterated chloroform (CDCl$_3$) as the solvent with tetramethylsilane as an internal standard. Surface morphology of the dendritic star copolymer was studied by atomic force spectroscopy (AFM) using a Veeco NanoMan V model. The AFM experiment was performed with a silicon tip at a spring constant of 1-5 N/m and resonance frequency of 60-100 kHz.

3,4-ethylenedioxy thiophene, generation 2 poly(propyleneimine) (G2PPI) dendrimer, 2-thiophene aldehyde and lithium perchlorate were purchased from Sigma-Aldrich (South Africa) as analytical grade chemicals. Deionized water

(18.2 MΩ) purified with a milli-Q™ system (Millipore) was used the preparation of solutions.

2.2. Synthesis of the G2 poly(propylene thiophenoimine) (G2PPT) dendrimer

The synthesis of G2PPT dendrimer was carried out by a condensation reaction of G2PPI with 2-thiophene aldehyde following the methods of Smith and his co-workers [31] and Salmon and Jutzi [32] with some modifications.

A reaction mixture of G2PPI dendrimer (2.68 g or 3.5 mmol) and 2-thiophene aldehyde (3.11 g or 27.78 mmol) in a 50 mL dry methanol was stirred continuously under a positive pressure of nitrogen gas for 2 days in a 100 mL three-necked round-bottom flask. The methanol was removed from the reaction mixture with a rotatory evaporator.

The residual oil was dissolved in 50 mL dichloromethane (DCM), while the organic phase was washed 8 times with 50 mL of water to remove any unreacted monomer. DCM was removed by rotary evaporation and the product was obtained as yellow oil.

Int. J. Electrochem. Sci., Vol. 6, 2011

1858

Scheme 1

2.3. Electrochemical synthesis of poly(propylene thiophenoimine)-co-poly(3,4 ethylenedioxythiopene)

(G2PPT-co-PEDOT) modified gold electrode.

A 2 mm diameter Au disk electrode was carefully polished to a mirror-like surface with

alumina powder of sizes 1.0, 0.3 and.05 μm, sequentially. Then the electrode was cleaned with piranha

(30% H_2O_2:H_2SO_4, 1:3) for 10 min at 80 °C in an oven followed by sonication in ethanol and water

consecutively for 5 min. The electrode was further cleaned electrochemically in 1 M sulphuric acid by

cycling between the potential of -200 mV to +1,500 mV until a reproducible cyclic voltammogram

was obtained. Subsequently the electrode was rinsed with copious amount of water, then absolute

ethanol and dried with nitrogen gas. 6 μL of 10 mg/mL G2PPT dendrimer was drop coated on the

cleaned Au electrode and left to dry for 12 h. The modified electrode was immersed into an aqueous

Int. J. Electrochem. Sci., Vol. 6, 2011

1859

solution of 0.1 M $LiClO_4$ containing 0.1 M 3,4-ethylenedioxylthiopene and 0.1 M sodium dodecyl sulphate by cycling the potential between -1,000 mV to +1,000

mV at a scan rate of 50 mV/s for ten cycles to obtain G2PPT-co-PEDOT (scheme 1).

3. RESULT AND DISCUSSION

3.1. Nuclear magnetic resonance (NMR)

The yield of the thiophene functionalized dendrimer, poly(propylene thiophenoimine), shown in Scheme 1, was 1.55 g, 68%. The $_1$HNMR (CDCl$_3$ 200 MHz, ppm) data for G2PPT are 1.40(s,br,4H,H-1), 1.78(t8H,H-2), 2.40(m,br,12H,H-2&3), 3.53(t,8H), 7.04(t,8H,H-8), 7.23(s4H,H-7), 7.26(s,4H,H-6), 7.82(C$_4$H$_3$S).

Figure 1. Fourier transforms infrared spectra of spectroscopy of G2PPT-co-PEDOT and G2PPT

The G2PPT $_1$HNMR spectra showed a new chemical shift at 8.37 ppm for C=N-H which is not shown in the parent G2PPI. Strong FTIR band (shown in fig 1) at 1622 cm$_{-1}$was observed which may be attributed to the formation of C=N-H bond in the dendrimer moiety while out of plane vibration for thiophene ring was obtained at 788 cm$_{-1}$ which corresponds to earlier reports [33-34]. The spectrum of the G2PPT showed an out of plane C-H bending located at the α-position of the thiophene ring observed at 722 cm$_{-1}$ which disappears after the polymerization, indicating that G2PPT was converted to G2PPT-co-PEDOT via α-α coupling of thiophene units

3.2. Atomic force microscopy analysis

AFM analysis was carried out on homopolymer and copolymer (G2PPT-co-PEDOT) in order to investigate the difference in their surface morphology so as to confirm the linking of the dendrimer moiety to the conducting polymer (PEDOT). The morphology in fig 2A showed smoothness at the surface due to the absence of dendrimer moiety. G2PPT-co-PEDOT modified electrode surface revealed a rough surface with formation of globular structure of different sizes which may be attributed to characteristic features of a dendrimer after electrochemical synthesis of G2PPT-co-PEDOT. The result confirmed the formation of copolymer (fig 2B) due to the incorporation of dendrimer moiety with conducting polymer (PEDOT) which was also corroborated by the globular structure obtained in SEM images for functionalized dendrimer alone. The 3D structure of G2PPT-co-PEDOT provides an appropriate coverage having dome-shaped dendrimer island structures with tiny holes appearing in the middle, which differ from PEDOT morphology and thereby demonstrating that G2PPT-co-PEDOT was deposited on the electrode surface.

A)

2D image of PEDOT 3D image of PEDOT

B)

2D image of G2PPT-co-PEDOT 3D image of G2PPT-co-PEDOT

Figure 2. Atomic force microscopy (AFM) images of (A) PEDOT, (B) G2PPT-co-PEDOT

Int. J. Electrochem. Sci., Vol. 6, 2011
1861

3.3. Scanning electron microscopy (SEM)
Figure 3 shows the scanning electron micrographs of (A) G2PPT, (B) PEDOT and (C) G2PPTco-
PEDOT electrode surface respectively. The morphology of the G2PPT, showed a homogeneous
globular formations on the electrode surface, quite different from the PEDOT film morphology that
exhibited flaky appearance. A significantly different morphology was observed for star copolymer
(G2PPT-co-PEDOT) which may be attributed to the enlargement of the globular structures of the
dendrimer moiety by the growth of the PEDOT arms, which may be considered as a further proof of
copolymerization.
(A) G2PPT (B) PEDOT film (C) G2PPT-co-PEDOT
Figure 3. Scanning electron micrographs of dendritic star polymer and its constituents.

3.4. Voltammetry of G2PPT-co-PEDOT
The cyclic voltammograms (CVs) of G2PPT-co-PEDOT modified electrode in 0.1 M LiClO$_4$ at
different scan rates ranging from 40-120 mV/s are shown in fig 4. The anodic peak current of G2PPTco-
PEDOT electrode is linearly dependent of the scan rate ( ) giving a regression equation i_{pa} (μA) = -
61.994 + 14.808X (r$_2$= 0.996).
This reveals that the electrode contains a thin electroactive surface-bound polymer film and the
occurrence of electron diffusion along the conducting dendritic star copolymer chain. The nature of the
process controlling the peak was elucidated from a plot of the log of anodic current (log i_{pa}) against the
log of scan rate (log) which gave a slope of 1.02, thus confirming an adsorption-controlled
electrochemistry of G2PPT-co-PEDOT nanoelectrode in 0.1 M LiClO$_4$. Integration of the CV of the
oxidation peak to obtain the amount of charge (C) involved in the reaction and substituting

appropriately in the Laviron equation [35-36], showed that the star polymer's electrochemistry is a

two-electron process. The surface concentration (Γ) of the G2PPT-co-PEDOT film was estimated to

be 1.96 x10^{-10} mol cm^{-2}, which was found to be higher than what was reported for other PEDOT

Int. J. Electrochem. Sci., Vol. 6, 2011

1862

copolymers on GCE electrode [37-38]. This Γ value in impedimetry analysis represents 97.3%

coverage.

Figure 4. Cyclic voltammetry of star copolymer Au|G2PPT-co-PEDOT at potential scan rates of 40 -

120 mV/s in 0.1 M LiClO$_4$.

3.5. Elecrochemical impedance spectroscopy (EIS) of G2PPT-co-PEDOT 0.1 M LiClO$_4$.

The dependance of the EIS parameters of the conducting polymer systems on applied potential

may be used to study the chacteristics of the film structures and kinetics, as well as the mechanisms for

charge transfer and ion transport in polymer film|electrolyte interface. However, impedance

spectroscopy also allows the detection of change in capacitance due to electrode modification. The low

frequency capacitance change (values) can be obtained from the imaginary part Z$_{im}$ of the complex

impedance part of the spectra using the following equation [30,39-41]

$$C_s = \frac{1}{2\pi f z_{im}}$$

(where f = maximum frequency, π = 3.142, Z$_{im}$ = slope of the plot of the imaginary impedance against

the reciprocal of frequency). The Nyquist plot for various modified electrodes showed a specific

capacitance of 26.5, 133.7 and 135.9 μF/cm$_2$ for bare Au, Au|PEDOT and Au|G2PPT-co-PEDOT,

respectively.

Int. J. Electrochem. Sci., Vol. 6, 2011

1863

Scheme 2. Redox species of G2PPT-co-PEDOT.

Figure 5 shows the Nyquist plot of bare gold electrode measured at different dc potential from –
600 to –1000 mV. However, both the impedance and phase angle do not exhibit distinctive response at
positive potentials up till +1000 mV open circuit.

Int. J. Electrochem. Sci., Vol. 6, 2011

1864

That is the reason for applying only negative potentials in the impedance study. As shown in
fig 5a, at –600 mV the Nyquist plot is characterized by the least semicircle compared to other
potentials indicating the occurrence of a charge tranfer process at the bare electrode.
The optimal potential was found to be –600 mV as can be seen in fig 5 which was further
coroborated by impedance plot in fig 5a. As the electrode potential was increased to positve values, a
switch to diffusion-controlled process was observed characterized by disappearance of semi circle.

A)

B) C)

Figure 5. (A) Randles equivalent circuit, (B) Nyquist and (C) Bode plots of the EIS data of bare Au in
0.1 M LiCLO$_4$ at different potentials.

Upon surface modification of gold electrode with G2PPT-co-PEDOT by
electrocopolymerization, the total impedance decreased with drastic drop in the value of the charge
tranfer resistance (fig 7) which is an indication of the polymerization of the EDOT monomer on the
dendrimer's thiophenoimine arms.
The most conducting potential was determined by interrogating the EIS of the star copolymer
at different potentials. As shown in fig 6a the most conducting potential was found to be –600 mV
which was taken as the optimal potential.

Int. J. Electrochem. Sci., Vol. 6, 2011

1865

A)

B)

Figure 6. Nyquist (A) and Bode (B) plots for Au│G2PPT-co-PEDOT at different potentials. Inset shows Nyquist plots at –800 to –600 mV.
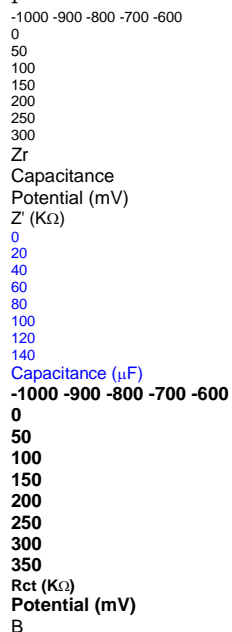
Figure 7. Nyquist plot diagrams for (a) bare Au (b) Au|PEDOT (c) Au|G2PPT-co-PEDOT at a

potential of -600 mV in 0.1 M LiClO4.

-1000 -900 -800 -700 -600
0
50
100
150
200
250
300
Zr
Capacitance
Potential (mV)
Z' (KΩ)
0
20
40
60
80
100
120
140
Capacitance (μF)
-1000 -900 -800 -700 -600
0
50
100
150
200
250
300
350
Rct (KΩ)
Potential (mV)
B
(A) (B)

Figure 8. Potential dependence of (A) real impedance and capacitance; and (B) charge transfer

resistance, for Au|G2PPT-co-PEDOT at 100 mHz.

As shown in fig 7 the diameter (i.e. charge transfer resistance, R_{ct}) of Nyquist semicircle was

smaller for Au|G2PPT-co-PEDOT ($7.805 \times 10_2$ Ω) than for bare Au ($2.907 \times 10_4$ Ω). This reavealed

the fact that the conducting PEDOT arms of the dendrimer facilitated the flow of charge through the

star copolymer onto the surface of the electrode. (see scheme 2). Also the PEDOT-modified electrode

gave a Nyquist semicircle diameter of $8.85 \times 10_2$ Ω, which was higher than the value of $7.805 \times 10_2$ Ω

obtained for Au|G2PPT-co-PEDOT. The increase in the conductivity of the dendritic star copolymer may also be attributed to the increase in the conjugation length of the copolymer after the incorporation of the PEDOT arms onto the dendrimer thereby facilitating easy flow of charge through the star copolymer and to the electrode surface.

The interfacial charge transfer resistance values, denoting either the kinetic resistance to charge transfer at the copolymer|solution boundary or electron tranfer at Au|G2PPT-co-PEDOT boundary, at different potentials were also ploted as shown in fig 8.

The charge storage capacity, the real impedance and the charge transfer resistance of Au|G2PPT-co-PEDOT varied with potential at the lowest fequency of 100 mHz as shown in fig 8. The optimum potential at which the dendritic star copolymer was more conductive was -600 mV with a charge storage capacity of 135 μF/cm$_2$ and lowest interfacial electron tranfer resistance as shown in fig 8. However, similar responses were obtained for bare Au and Au|PEDOT at the same potential of -600 mV used for comparing the behaviour of the three electrode platforms as illustrated by the Nyquist plots shown in fig 7. Kinetic parameters of the electrode systems, e.g. time constant (τ), exchange current (i_o) and heterogeneous rate constant (k_{et}) were estimated so as to ascertain the catalytic and conductivity behavior of the dendritic star copolymer on the kinetics of the supporting electrolyte [38-39]. The τ values were 4.7 x 10$_{-2}$ s rad$_{-1}$, 1.64 x 10$_{-5}$ s rad$_{-1}$ and 1.45 x 10$_{-5}$ s rad$_{-1}$ for bare Au, Au|PEDOT and Au|G2PPT-co-PEDOT, respectively. The i_o value for the charge transfer from star copolymer film to the electrode surface was 1.64 x 10$_{-5}$ A which is higher than the values for bare Au (4.40 x 10$_{-7}$ A) and Au|PEDOT (1.45 x 10$_{-5}$ A).

These results show that the flow of charge through the star copolymer onto the surface of the electrode is faster at the Au|G2PPT-co-PEDOT modified electrode than the bare electrode. Heterogeneous rate constant is a measure of the rate of electron transfer on the surface of the electrode. Thus, an increase in k_{et} value from 1.09 x 10$_{-6}$ cm s$_{-1}$ for bare Au electrode to 4.05 x 10$_{-5}$ cm s$_{-1}$ for the dendritic star copolymer modified electrode also corroborated the facile flow of charge through the copolymer platform [42-43]. Besides, the time constant obtained (table 1) for the star copolymer platform was lower than that for the bare Au electrode, which is in agreement with earlier reports for modified electrodes [42-43]. The impedance parameters in table 1 were obtained by fitting the equivalent circuit shown in fig 5A and the fitting error was less than 5% .

Table 1. Kinetic parameters of the modified electrode systems.

Exchange current (i_o, A)
4.40 x 10$_{-7}$
1.45 x 10$_{-5}$
1.64 x 10$_{-5}$
Heterogeneous rate constant(k_{et}, s$_{-1}$)
1.09 x 10$_{-6}$

3.58 x 10^{-5}

4.05 x 10^{-5}

Time constant (τ, s rad^{-1})

4.70 x 10^{-2}

1.15 x10^{-2}

1.49 x 10^{-3}

Besides changes in the total impedance, changes were also observed in the phase angle values after gold electrode was modified with PEDOT and G2PPT-co-PEDOT. Figure 9 shows the plots of

Int. J. Electrochem. Sci., Vol. 6, 2011

1868

phase angle changes with frequency for the bare Au, PEDOT and G2PPT-co-PEDOT. Bode plots showed remarkable differences in the electronics of bare Au, PEDOT and G2PPT-co-PEDOT interfaces. The frequency of maximum phase angle increased from bare Au to PEDOT and G2PPT-co-PEDOT with the phase angle decreasing from semi-metallic value for Au (70°) to semiconductor value for PEDOT (25°) and G2PPT-co-PEDOT (20°), which is in agreement with earlier reports [30, 39].

Figure 9. Bode phase angle plots of Au|G2PPT-co-PEDOT star co-polymer and its components.

On the other hand the EIS spectra show that at low frequency (100 mHz.) when the electronic of the electrode system are minimally perturbed, the Au|G2PPT-co-PEDOT exhibited semi metallic behavior (phase angle value of 67.5°) while Au|PEDOT (with a phase angle values of 52.9°) showed semiconductor behaviour.

4. CONCLUSIONS

A novel dendritic star copolymer, G2PPT-co-PEDOT, which was successfully synthesized electrochemically was found to exhibit high conductivity which facilitated the flow of charge through the conducting co-polymer. Morphological characterization of G2PPT-co-PEDOT revealed a globular

Int. J. Electrochem. Sci., Vol. 6, 2011

1869

porous structure which explains the ease of charge transportation through the copolymer film. The electrochemistry of the nanoelectrode showed a two electron process, while the Bode phase angle analysis of EIS data confirmed that the copolymer is a highly conducting semiconductor.

References

1. T.A. Skotheim, R.L. Elsenbaumer and J.R. Reynolds (Eds.), *Handbook of Conducting Polymers*, 2nd Edition, Marcel Dekker. Inc., New York (1998).
2. L. Groenendaal, F. Jonas, D. Freitag, H. Pielartzik and J.R. Reynolds, *Adv. Mater.*, 12 (2000) 481.

3. G. Sonmez, P. Schottland and J.R. Reynolds, *Synth. Met.*, 155 (2005) 130.

4. V.S. Vasantha, R. Thangamuthu and S-M. Chen, *Electroanal.*, 20 (2008) 1754.

5. N. Rozlosnik, *Anal. Bioanal. Chem.*, 395 (2009) 637.

6. R. Ruffo, A. Celik-Cochet, U. Posset, C.M. Mari and G. Schottner, *Sol. Energ. Mat. Sol. C.*, 92 (2008) 140.

7. P. Damlin, C. Kvarnström and A. Ivaska, *J. Electroanal. Chem.*, 570 (2004) 113.

8. W.A. Gazotti Jr, G. Casalbore-Miceli, S. Mitzakoff, A. Geri, M.C. Gallazzi and M.A. De Paoli, *Electrochim. Acta*, 44 (1999) 1965.

9. M. Higuchi, Y. Akasaka, T. Ikeda, A. Hayashi and D. Kurth, *J. Inorg. Organomet. P.*, 19 (2009) 74.

10. B.C. Thompson, P. Schottland, K. Zong and J. R. Reynolds, *Chem. Mater.*, 12 (2000) 1563.

11. P-M. Carrasco, C. Pozo-Gonzalo, H. Grande, J.A. Pomposo, M. Cortázar, V. Deborde, M. Hissler and R. Reau, *Polym. Bull.*, 61 (2008) 713.

12. U. Bulut, F. Yilmaz, Y. Yagci and L. Toppare, *React. Funct. Polym.*, 61 (2004) 63.

13. E. Sahin, P. Camurlu, L. Toppare, V.M. Mercore, I. Cianga and Y. Yagci, *Electroanal. Chem.*, 579 (2005) 189.

14. J. Xu, G. Nie, S. Zhang, X. Han, J. Hou and S. Pu, *J. Mater. Sci.*, 40 (2005) 2867.

15. L.L. Miller, R.G. Duan, D.C. Tully and D.A. Tomalia, *J. Am. Chem. Soc.*, 119 (1997) 1005.

16. Z. Zhang, W. Yang, J. Wang, C. Yang, F. Yang, X. Yang, *Talanta*, 78 (2009) 1240.

17. O. A. Arotiba, P.G.L. Baker, B. B. Mamba, E. Iwuoha, *Int. J. Electrochem. Sci.* 6 (2010) 673.

18. T. Ndlovu, O. A. Arotiba, R. W. Krause, B.B. Mamba, *Int. J. Electrochem. Sci.*, 5 (2010) 1179

19. S. Deng, J. Locklin, D. Patton, A. Baba and R.C. Advincula, *J. Am. Chem. Soc.*, 127 (2005) 1744.

20. C. Xia, X. Fan, J. Locklin, R.C. Advincula, A. Gies and W. Nonidez, *J. Am. Chem. Soc.*, 126 (2004) 8735.

21. P.R.L. Malenfant, M. Jayaraman and J.M.J. Frechet, J. *Am. Chem. Soc.*, 11 (1999) 3420.

22. J.L. Hedrick, M. Trollsas, C.J. Hawker, B. Atthoff, H. Claesson, A. Heise, R.D. Miller, D. Mecerreyes, R. Jerome and P. Dubois, *Macromolecules*, 31 (1998) 8691.

23. J. Roovers, L.L. Zhou, P.M. Toporowski, M. Van Der Zwan, H. Iatrou and N. Hadjichristidis, *Macromolecules*, 26 (1993) 4324.

24. R.C. Hedden and B.J. Bauer, *Macromolecules,* 36 (2003) 1829.

25. Y. Zhao, X. Shuai, C. Chen and F. Xi, *Chem. Mater.*, 15 (2003) 2836.

26. A. Heise, S. Diamanti, J.L. Hedrick, C.W. Frank and R.D. Miller, *Macromolecules,* 34 (2001) 3798.

27. Q. Zheng and C.-Y. Pan, *Eur. Polym. J.,* 42 (2006) 807.

28. Q. Zheng and C.-Y. Pan, *Macromolecules,* 38 (2005) 6841.

29. J. Wang, M. Jiang, A. Fortes and B. Mukherjee, *Anal. Chim. Acta,* 402 (1999) 7.

Int. J. Electrochem. Sci., Vol. 6, 2011

1870

30. L. Niu, Q. Li, F. Wei, X. Chen and H. Wang, *J. Electroanal. Chem.,* 544 (2003) 121.

31. G. Smith, R. Chen and S. Mapolie, *J. Organomet. Chem.,* 673 (2003)

32. A. Salmon and P. Jutzi, *J. Organomet. Chem.* 637-639 (2001) 595.

33. H.X. Min, Z. Wei, Y.P. Xie and X.H. Ping, *Chinese Chem. Lett.,* 17 (2006) 1251.

34. Z. Wei, J. Xu, J. Hou, W. Zhou and S. Pu, *J. Mater. Sc,* 41 (2006) 3923.

35. E. Laviron, *J. Electroanal. Chem.,* 100 (1979) 263.

36. R. Greef, R. Peat, L.M. Peter, D. Pletcher and J. Robinson, Instrumental Methods in Electrochemistry, Ellis Horwood Limited, New York (1990).

37. R. Zhang, G. Dijin, D. Chen and X. Hu, *Sensor and Acuat.B-Chem.,* 138 (2009) 174.

38. A. Balamurugan and S.-M. Chen, *Sensor and Acuat.B-Chem.,* 129 (2008) 850.

39. A.S. Sarac, M. Ates and B. Kilic, *Int. J. Electrochem. Sci.,* 3 (2008) 777

40. M. Ates, *Int. J. Electrochem. Sci.,* 4 (2009) 1004

41. E. Katz and I. Willner, *Electroanal.,* 15 (2003) 913.

42. R.A. Olowu., O. Arotiba., S.N. Mailu., T.T. Waryo., P. Baker and E. Iwuoha, *Sensors,* 10 (2010) 9872.

43. O.A. Arotiba, J.H. Owino, P.G. Baker and E.I. Iwuoha, *J. Electroanal. Chem.,* 638 (2010) 287.